Extinction coefficients retrieved in deep tropical ice clouds from lidar observations using a CALIPSO-like algorithm compared to in-situ measurements from the Cloud Integrated Nephelometer during CRYSTAL-FACE

Vincent Noel, D. M. Winker, T. J. Garrett, M. Mcgill

Atmos. Chem. Phys. Discuss., 6, 10649–10672, 2006
www.atmos-chem-phys-discuss.net/6/10649/2006/

Atmospheric Chemistry and Physics Discussions

Extinction coefficients retrieved in deep tropical ice clouds from lidar observations using a CALIPSO-like algorithm compared to in-situ measurements from the Cloud Integrated Nephelometer during CRYSTAL-FACE

V. Noel[1], D. M. Winker[2], T. J. Garrett[3], and M. McGill[4]

[1]Laboratoire de Météorologie Dynamique, Palaiseau, France
[2]NASA Langley Research Center, Hampton, VA, USA
[3]University of Utah, Salt Lake City, UT, USA
[4]NASA Goddard Space Flight Center, Greenbelt, ML, USA

Received: 10 February 2006 – Accepted: 26 April 2006 – Published: 19 October 2006

Correspondence to: V. Noel (vincent.noel@lmd.polytechnique.fr)

Abstract

This paper presents a comparison of lidar ratios and volume extinction coefficients in tropical ice clouds, retrieved using observations from two instruments: the 532-nm *Cloud Physics Lidar* (CPL), and the in-situ *Cloud Integrating Nephelometer* (CIN) probe. Both instruments were mounted on airborne platforms during the CRYSTAL-FACE campaign and took measurements up to 17 km. Coincident observations from two cases of ice clouds located on top of deep convective systems are compared. First, lidar ratios are retrieved from CPL observations of attenuated backscatter, using a retrieval algorithm for opaque cloud similar to one used in the soon-to-be launched CALIPSO mission, and compared to results from the regular CPL algorithm. These lidar ratios are used to retrieve extinction coefficient profiles, which are compared to actual observations from the CIN in-situ probe, putting the emphasis on their vertical variability. When observations coincide, retrievals from both instruments are very similar. Differences are generally variations around the average profiles, and general trends on larger spatial scales are usually well reproduced. The two instruments agree well, with an average difference of less than 11% on optical depth retrievals. Results suggest the CALIPSO Deep Convection algorithm can be trusted to deliver realistic estimates of the lidar ratio, leading to good retrievals of extinction coefficients.

1 Introduction

Cirrus clouds are high altitude clouds mostly composed of ice crystals. Since they consistently cover more than 30% of the earth's surface (Wylie et al., 1994), their influence the radiation budget cannot be overlooked (Stephens et al., 1990). The radiative influence of a given cirrus cloud depends mostly on the delicate balance between its albedo effect and its greenhouse effect. The dominant effect is globally unknown, and locally it depends on the microphysical and optical properties of the considered cirrus cloud. Most noticeably, the quantity of reflected sunlight reflected by a cirrus cloud (and

ACPD

6, 10649–10672, 2006

thus its albedo effect) is directly tied to its optical thickness τ, defined as $\tau = \int_{z_0}^{z_1} \alpha(z)dz$: the vertical integration of its extinction coefficient $\alpha(z)$ between the cloud boundaries z_0 and z_1. The albedo of a cloud is thus directly dependent on its vertical profile of extinction coefficient. A good knowledge of extinction coefficients, and thus optical depth, in cirrus clouds would lead to a better estimation of their general albedo effect.

Due to the high altitude of cirrus clouds, direct in situ measurement of their microphysical properties is a difficult task that cannot be pursued on a systematic basis. Moreover, in the tropics ice clouds are often located on top of deep convective systems (see e.g. Garrett et al., 2004), which means high-altitude observations are a necessity. Because of their large horizontal and vertical extensions, these systems have a large-scale radiative impact on the planet surface and atmosphere (Hartmann et al., 1992), and their creation through fast convection leads to specific microphysic and optical properties (McFarquhar and Heymsfield, 1996; Heymsfield and McFarquhar, 1996). Unfortunately, when conducting satellite studies using passive remote sensing it is often difficult to separate an optically thin ice cloud layer from an underlying convective system, meaning high uncertainties in the retrievals (Chiriaco et al., 2004). This stresses the need for active remote sensing, such as lidar, whose sensitivity to optically thin clouds makes it one of the most appropriate instruments for cirrus study (Platt, 1973) and can give valuable insights into ice cloud microphysics (Noel and Chepfer, 2004; Noel et al., 2004). Lidar retrievals of extinction coefficients are an effective tool for studying the optical depth of ice clouds out of reach of in-situ observations, and are not subject to passive remote sensing limitations, as the variability of extinction coefficients is observed as a function of penetration inside the cloud layer. Moreover, the upcoming launch of a 532-nm lidar on a spaceborne platform in the framework of the CALIPSO mission (Winker et al., 2003) will lead to retrievals of extinction coefficients and thus optical depths on a global scale, even for tropical ice clouds on top of optically thick convective systems.

In the present study, attenuated backscatter profiles observed in deep tropical ice

ACPD
6, 10649–10672, 2006

EGU

clouds using the *Cloud Physics Lidar* (CPL) on 28 and 29 July during the *Cirrus Regional Study of Tropical Anvils and Cirrus Layers – Florida Area Cirrus Experiment* (CRYSTAL-FACE, Jensen et al., 2004) are used to retrieve lidar ratios, using the CALIPSO "Deep Convection" retrieval algorithm (Winker, 2003). Results are compared to retrievals using the regular CPL algorithm, then with actual in-situ observations from the airborne collocated probe *Cloud Integrating Nephelometer* (CIN, Garrett et al., 2003). The CRYSTAL-FACE campaign is presented in Sect. 2, along with the instruments used by the present study. The CALIPSO Deep Convection retrieval algorithm is presented and its results compared with results from the CPL algorithm in Sect. 3. Lidar ratio retrievals are then used to retrieve extinction coefficient profiles in Sect. 4, which are compared to in-situ CIN observations. Discussion and conclusion are given in Sect. 5.

2 Volume extinction coefficient retrievals during CRYSTAL-FACE

The CRYSTAL-FACE campaign was held in July 2002 over Florida and the Gulf of Mexico, and aimed to provide the comprehensive measurements needed to better understand the microphysical and radiative properties and formation processes of ice clouds on top of thick convective cloud systems. Five mid- to high-altitude aircraft carried numerous in situ and remote sensing instruments, with simultaneous ground-based observations. Among these, the NASA *Cloud Physics Lidar* CPL, a three-wavelength (355 nm, 532 nm and 1064 nm) backscatter lidar (McGill et al., 2002), was looking downward from the NASA ER-2 aircraft (King and al., 2003) and provided several days of observations from as high as 20 km, with a vertical resolution of 30 m and an horizontal resolution of approximately 200 m at the typical ER-2 flying speed of 200 m.s^{-1}. The CPL telescope field of view is 100 μradians, so the footprint on a cloud located less than 10 km away (the typical distance during CRYSTAL-FACE) would be less than 1 m wide. This configuration allowed unique monitoring of ice clouds located on top of tropical convective systems, which would be impossible from the ground be-

ACPD
6, 10649–10672, 2006

cause of the lower layers of thick water clouds blocking the lidar penetration. From the raw backscattered laser light measured by the CPL telescope, properties of cloud and aerosol layers are retrieved, including the altitude of cloud base and cloud top, its optical depth τ, and profiles of depolarization ratio and volume extinction coefficient. The method used for analysis and retrieval of the volume extinction is explained in McGill et al. (2003), and is based on the standard lidar inversion technique (e.g. Spinhirne et al., 1980; Klett, 1981). When possible (i.e. for optically thin clouds), the lidar extinction-to-backscatter ratio S (Sect. 3.1) is retrieved directly from lidar observations (through a transmission-loss technique). When this is not possible (i.e. for optically thick clouds such as convective systems), $S$is provided below –13°C by a quadratic function of temperature: $S=aT^2+bT+c$ with $a=-1.42739e-3$, $b=-2.08944e-1$ and $c=1.5339e+1$ at a wavelength of 532 nm (a different quadratic function is used at 1064 nm). For temperatures warmer than –13°C, a value $S=17.84$ is used (D. L. Hlavka, private communication, 2005). A very similar technique is used when analyzing observations from the spaceborne *Geoscience Laser Altimeter System* (Zwally et al., 2002).

The CIN probe was mounted on the WB-57 aircraft, which was able to fly through the top of tall convective systems thanks to its high ceiling (up to 18km). The CIN measures extinction coefficients from the scattering of cloud particles of a 635 nm laser light into sensors, consisting of circular light-diffusing disks and photomultipliers (Gerber et al., 2000). These sensors measure the forward-scattered and backscattered light between 10° and 175°, from which the volume extinction parameter is inferred based on an estimate of the light forward-scattered by diffraction (Eq. 7 in Gerber et al., 2000). Since diffraction is necessarily one half of scattered energy, the omitted fraction is constrained and is estimated to be 0.57±0.02. The estimated uncertainty in the extinction coefficient during CRYSTAL-FACE was 15%.

ACPD
6, 10649–10672, 2006

3 The CALIPSO deep convection algorithm

3.1 Lidar ratio retrieval

For elastic backscatter lidars, volume extinction coefficient profiles $\alpha(z)$ are retrieved from observations of attenuated backscatter profiles $\beta(z)$. In order to do so, a relationship between the backscatter and extinction coefficients must be assumed. Often defined as $S=\frac{\alpha}{\beta}$, the lidar ratio, this relation is assumed to stay constant within a cloud layer.

The magnitude of the lidar ratio depends on the microphysical properties of the cloud, but in many cases can be retrieved from attenuated backscatter observations alone. In the routine analysis of CALIPSO observations, different algorithms are used depending on the opacity of the atmospheric layer. For semi-transparent clouds, a transmittance algorithm is used, based on the difference in lidar return signal from clear regions above and below the cloud layer. In the case of fully attenuating layers, such as deep tropical thick convective systems, the transmittance algorithm cannot be applied, as the laser cannot penetrate the layer fully and no signal is available beyond the cloud layer. An equation can be derived which relates the cloud-integrated attenuated backscatter signal γ' to the cloud transmittance T (Platt, 1973; Platt et al., 1999):

$$\gamma' = \frac{1 - T^2}{2S\eta} \tag{1}$$

where η is a multiple scattering correction factor. In the case of an opaque cloud layer, $T=0$ so that $\gamma'=\frac{1}{2S\eta}$. The lidar ratio can thus be retrieved from lidar profiles of attenuated backscatter and an estimate of η. This is the essence of the algorithm used by CALIPSO to retrieve extinction in the tops of deep convective clouds (Winker, 2003).

ACPD
6, 10649–10672, 2006

EGU

3.2 Lidar ratio retrieval on 29 July

On 29 July, a CRYSTAL-FACE mission focused on a small-scale convective system (McGill et al., 2004) that extended horizontally over 100 km and up to the tropopause (higher than 14 km), meaning the highest several kilometers were composed of ice crystals. CPL observations of attenuated backscatter between 19:18 and 19:42 are shown in Fig. 1 as a function of time and altitude, on a logarithmic color scale. During this timeframe, the ER-2 carrying the CPL flew over the convective system in a straight line, and CPL observations show the top of the system rises from 12 km at its edges to more than 14 km in its central area, close to the convective center. The CPL was able to penetrate the cloud layer at least one kilometer before the laser signal was completely attenuated (Fig. 1), but coincident observations from the *Cloud Radar System* (not shown, Li et al., 2004), also mounted on the ER-2, show this cloud system extended down to the surface.

The lidar ratios retrieved during the same timeframe are shown in Fig. 2, using the CPL algorithm (in black) and the CALIPSO Deep Convection algorithm described above (in red). Because of the small field of view of the CPL instrument and the nearness of the cloud, multiple scattering is insignificant, and the lidar ratio is retrieved simply as $S=1/2\gamma'$. The two sets of values are very similar, most in the 20–40 range, with some outlier points up to 80. In the opaque portions of the cloud, the agreement is very good; near the cloud edges (not opaque), values derived using the Deep Convection algorithm are too large. In this case, the CALIPSO operational code uses a more appropriate transmittance-based retrieval.

The same comparison was conducted on all cloud layers detected on 29 July, and on similar observations made on 28 July. The average difference and its standard deviation are shown on a logarithmic scale in Fig. 3, as a function of the minimum considered optical depth τ_{min}. When considering all cloud layers (τ_{min}=0), the average difference goes as high as 100 for 28 July, showing the Deep Convection algorithm leads to unrealistic results in such conditions, as expected. However, as τ_{min} increases,

ACPD
6, 10649–10672, 2006

the difference quickly decreases below 10 for τ_{min}=0.3 (29 July) and τ_{min}=1 (28 July), down to 2 (29 July) and 1 (28 July) for τ_{min}>2. The standard deviation simultaneously goes through the same decrease, dropping from values greater than 100 to less than 5. The decrease is especially important for 28 July. Figure 3 shows that the CALIPSO Deep Convection algorithm is well suited to the study of optically thick cloud layers.

3.3 Extinction retrieval

Using the CPL attenuated backscatter observations (Sect. 3.1) and the retrieved lidar ratios (Sect. 3.2), it is possible to retrieve the actual particulate backscatter $\beta(z)$ at the altitude z from the well-known forward solution to the lidar equation (Platt et al., 1973):

$$\beta(z) = \frac{\beta'(z)}{1 - 2\eta S \int \beta'(z')\, dz'} \tag{2}$$

with $\beta'(z)$ the observed attenuated backscatter, and z_0 the altitude of lidar penetration in the layer (i.e. the cloud top for a nadir-looking lidar like the CPL). As the goal of this study is an operational validation of the CALIPSO Deep Convection algorithm (Sect. 3.1), a simple application of this algorithm will provide a good first approximation for comparison purposes. Once backscatter profiles $\beta(z)$ are retrieved, extinction coefficients $\alpha(z) = \beta(z) \cdot S(z)$can be easily obtained for any given layer (Sect. 3.1). This technique was applied to CPL observations of attenuated backscatter in ice clouds from 28 and 29 July (Sect. 3.2). Results of these retrievals will be presented and compared to in-situ probe observations in the next section.

4 Coincident observations of extinction in cirrus clouds

During CRYSTAL-FACE, cirrus clouds were observed many hours by the CPL (on the ER-2) and the CIN (on the WB-57), but most of the time the observations were not simultaneous. This part of the study will focus on the periods of time when the two

instruments were functioning simultaneously and their two aircraft were flying in the same area, so that the two instruments were monitoring the same cloud. To evaluate the variability of extinction with altitude, and the correlation between results from both instruments, only cases when the WB-57 was either climbing or descending in the cloud layer were considered. Periods of observation fitting this description for 28 and 29 July are described in Table 1. For each CPL profile, coordinates of the supporting ER-2 aircraft were compared to those of the WB-57 in the timeframe of coincidence, the maximum delay between both aircraft being 6 min.

As seen in Sect. 3.2, the 28 and 29 July cases are typical of the small-scale convective systems that developed frequently in the tropical area monitored during CRYSTAL-FACE. Volume extinction coefficients retrieved from CPL backscatter observations using the CALIPSO Deep Convection algorithm (Sects. 3.1 and 3.3) are shown in Fig. 4 (28 July) and Fig. 5 (29 July), with the WB-57 altitude at coincident points plotted over in red symbols. On 28 July, the lidar penetration depth is very variable on time scales of less than a minute: most profiles are fully attenuated before the signal reaches 13 km; however some isolated profiles show deeper penetration and reach 13 km (e.g. around 22:57). This seems due to rapid small-scale variations in the spatial distribution of cloud water content. The extinction coefficient is generally in the 10^{-3} to 3.10^{-3}m^{-1} range (green on the color scale). The studied timeframe on 29 July (Fig. 5) shows a stable lidar penetration depth, 1 km on average, but is less homogeneous, with wider variations in retrieved extinction values (from 5.10^{-4} to 10^{-2} m^{-1}). Integrating these extinction profiles gives a highly variable time series of optical depths (not shown), with values typically ranging between 1 and 4. As the optical depth approaches these higher values, the retrievals become unreliable for two reasons: 1) it is well known that the forward solution becomes unstable at high optical depths and can become divergent (Platt et al., 1987), and 2) the backscatter return signal becomes very weak and noise excursions influence the retrieved values. Thus extinction coefficients at low altitudes, such as the very high extinctions at the largest penetration depths (red on the color scale in Figs. 4 and 5) should be treated with caution.

ACPD
6, 10649–10672, 2006

For each CPL profile, extinction coefficients were extracted from the CIN data at the point of closest WB-57 and ER-2 coincidence. On 28 July, the WB-57 went from 16 km at 22:45 down to 13 km around 23:00 (Fig. 4). To sample the maximum of cloud data during descent, the WB-57 was often spiraling inside cloud systems, which is why these points are not in chronological order. The extinction observed by the CIN during this period is shown as symbols in Fig. 6 as a function of altitude, with horizontal bars showing the uncertainty. The average extinction profile retrieved from CPL observations during the same timeframe is shown in full line, the shaded area showing the standard deviation around the average. The agreement between both instruments is good between 13.7 and 15 km, with an average difference of 0.166 10^{-2} between profiles, which implies that the Deep Convection algorithm is choosing appropriate values for S. Profiles are clearly different below 13.7 km, where the lidar still sees large extinction (up to $10^{-2}\,m^{-1}$) down to 13.0 km where the signal is totally attenuated (radar data shows the cloud base was actually much lower), while extinction from the CIN probe falls to zero around 13.7 km. These differences could be due to local variations encountered by the WB-57 during its descent, or to the WB-57 flying into a cloud-free region. Integrating both CPL and CIN profiles of extinction coefficient over the correlated regions (13.7 to 15 km) leads to respective optical depths τ of 1.87 and 1.67 (Table 2), i.e. the CPL-derived value is 11% larger than the CIN-derived value, within the measurement uncertainties of the two instruments. Integrating the CPL extinction profile over the full layer (i.e. 13 to 15 km) gives a much higher value of τ=4.6. This is a very high optical depth for a lidar to penetrate, and indicates the variability of the profile below about 13.7 km may be due to weak signal and the lowest part of the profile is probably unreliable. The CIN detects some low extinction coefficients (α<$10^{-3}\,m^{-1}$) at the tropopause level (15.5 km according to radiosoundings launched at 23:00 from Tampa, 27.70° N, 82.40° W) that do not appear in the lidar retrievals (Fig. 6); these values are below the CIN noise level and should not be considered as actual particles.

On 29 July, the WB-57 went from 14 km at 20:00 down to 12.5 km at 20:12 (red symbols in Fig. 5). A comparison of extinction profiles (Fig. 7) shows that once again

ACPD
6, 10649–10672, 2006

retrievals on CPL data using the CALIPSO Deep Convection algorithm are very similar to CIN observations. Consistent with Fig. 5, high extinction coefficients (larger than $5.10^{-3}\,m^{-1}$) are observed. Both profiles are in good agreement from cloud top (14 km) down to 12.5 km, where CIN measurements suddenly drop to zero, suggesting the WB-57 moved in a cloud-free region. The simultaneous sudden break in lidar observations at 12.5 km is due to total signal attenuation, as radar observations show a lower cloud base. As in the 28 July case, CPL retrievals are highly variable at low altitudes (e.g. below 13 km), due to weak signal and the limited stability of the inversion algorithm. Integration of extinction profiles leads to very high optical depths (Table 2): 4.74 and 5.08, respectively for the CPL and the CIN. These values are consistent with the full-profile optical depth for 28 July (4.6). The slightly lower optical depth from CPL extinctions is consistent with total lidar signal attenuation.

5 Discussion and conclusion

This study presents a comparison between volume extinction coefficients observed from a CIN in-situ probe and retrievals from lidar backscattering profiles (Sect. 2). Three coincident observation periods are compared, highlighting the variability with altitude (Sect. 4). Results show a very good agreement between both instruments, for extinction coefficients sometimes as low as $10^{-3}\,m^{-1}$ (Fig. 2). This implies the CALIPSO Deep Convection algorithm is doing a good job at selecting lidar ratios for opaque clouds. Overall the extinction coefficient profiles retrieved from CPL observations show higher small-scale variability (in the 100-m range) than the CIN observations. This may be due to the unstable nature of the extinction retrieval algorithm at high optical depths, which creates large fluctuations in backscattering coefficient from one profile to the next. However, CIN observations are often contained within the standard deviation of CPL retrievals. As variations on larger scales are well reproduced, the retrieved optical depth is only slightly affected (6 and 11% variations between the two instruments when considering intersecting observations). In the second case (29

ACPD
6, 10649–10672, 2006

July), the extinction coefficients retrieved from the lidar were slightly lower than those observed in-situ by the CIN. This can be explained by the lidar signal being fully attenuated by the optically thick layer of the convective systems, and thus unable to penetrate the whole cloud layer measured by the CIN. Overall, the lidar performs reasonably well in such extreme conditions (i.e. very thick convective system), and as it was shown previously those differences are only significant on small spatial scales and are only a secondary influence on larger scale trends and integrated results.

Recent comparisons between collocated in-situ probes during CRYSTAL-FACE (Heymsfield et al., 2006) suggest observations from the CIN might exhibit a bias towards smaller particles, thus leading to a possible overestimation of the extinction coefficient, potentially by as much as a factor of 2. Additional work might therefore be required to determine if the good agreement found between results from both instruments in the present study is the byproduct of distinct observational and analysis biases in each instrument, which would compensate for each other and coincidentally lead to similar results. On the other hand, the fact that results from both instruments, using very different techniques, show a good agreement strengthens the confidence in extinction coefficients retrieved from both instruments. Moreover, even in the case of a quantitative bias, the fact that the variations of extinction coefficient are similar with altitude in same-day profiles from each instrument still suggests the vertical variability of lidar retrievals can be trusted. In any case, retrievals from both instruments are consistent for low values of extinction (below 10^{-3} m^{-1}) that would still remain small after a numerical correction. The results are especially important since observations from the spaceborne CALIPSO mission (Winker et al., 2003) will soon be available, leading to an extensive mapping of ice cloud optical and microphysical properties.

Acknowledgements. This research was supported in part by the NASA Langley Research Center under contract NAS1-02058. The Cloud Physics Lidar is sponsored by NASA's Radiation Sciences Program and by NASA's Earth Observing System (EOS) office.

References

Chiriaco, M., Chepfer, H., Noel, V., Delaval, A., Haeffelin, M., Dubuisson, P., and Yang, P.: Improving Retrievals of Cirrus Cloud Particle Size Coupling Lidar and Three-channel Radiometric techniques, Mon. Wea. Rev., 132, 1684–1700, 2004.

Garrett, T. J., Gerber, H., Baumgardner, D. G., Twohy, C. H., Baumgardner, D. G., and Weinstock, E. M.: Small, highly reflective ice crystals in low-latitude cirrus, Geophys. Res. Lett., 30, doi:10.1029/2003GL018153, 2003.

Garrett, T. J., Heymsfield, A. J., McGill, M. J., Ridley, B. A., Baumgardner, D. G., Bui, T. P., and Webster, C. R.: Convective generation of cirrus near the tropopause, J. Geophys. Rev., 109, D21203, doi:10.1029/2004JD004952, 2004.

Gerber, H., Takano, Y., Garrett, T. J., and Hobbs, P. V.: Nephelometer measurements of the Asymmetry parameter, Volume extinction coefficient and Backscatter ratio in Artic clouds, J. Atmos. Sci., 57, 3021–3034, 2000.

Hartmann, D. L., Ockert-Bell, M. E., and Michelsen, M. L.: The effect of cloud type on earth's energy balance: Global analysis, J. Clim., 5, 1281–1304, 1992.

Heymsfield, A. J. and McFarquhar, G. M.: On the high albedos of anvil cirrus in the tropical pacific warm pool: microphysical interpretations from CEPEX and from Kwajalein, Marshall Islands, J. Atmos. Sci., 53, 2401–2423, 1996.

Heymsfield, A. J., Schmitt, C., Bansemer, A., Van Zadelhoff, G. J., McGill, M. J., Twohy, C., and Baumgardner, D.: Effective Radius of Ice Cloud Particle Populations Derived from Aircraft Probes, submitted, J. Atmos. Ocean. Tech., 23, 361–380, 2006.

Jensen, E. J., Starr, D., and Toon, O. B.: Mission investigates tropical cirrus clouds, EOS, 85, 45–50, 2004.

King, M. D., Platnick, S., Moeller, C. C., Revercomb, H. E., and Chu, D. A.: Remote sensing of smoke, land, and clouds from the NASA ER-2 during SAFARI 2000, J. Geophys. Res., 108(D13), 8502, doi:10.1029/2002JD003207, 2003.

Klett, J. D.: Stable analytical inversion solution for processing lidar returns, Appl. Opt., 20, 211–220, 1981.

Li, L., Heymsfield, G. M., Racette, P. E., Tian, L., and Zenker, E.: A 94-GHz cloud radar system on a NASA high-altitude ER-2 aircraft, J. Atmos. Oceanic. Technol., 21(9), 1378–1388, 2004.

McFarquhar, G. M. and Heymsfield, A. J.: Microphysical characteristics of three cirrus anvils

sampled during the Central Equatorial Pacific Experiment (CEPEX), J. Atmos. Sci., 52, 2401–2423, 1996.
McGill, M. J., Hlavka, D. L., Hart, W. D., Spinhirne, J. D., Scott, V. S., and Schmid, B.: The Cloud Physics Lidar: Instrument description and initial measurement results, Appl. Opt., 41, 3725–3734, 2002.
McGill, M. J., Hlavka, D. L., Hart, W. D., Welton, E. J., and Campbell, J. R.: Airborne lidar measurements of aerosol optical properties during SAFARI 2000, J. Geophys. Res., 108, 8493, doi:10.1029/2002JD002370, 2003.
McGill, M. J., Li, L., Hart, W. D., Heymsfield, G. M., Hlavka, D. L., Racette, P. E., Tian, L., Vaughan, M. A., and Winker, D. M.: Combined lidar-radar remote sensing: Initial results from CRYSTAL-FACE, J. Geophys. Res., 109, D07203, doi:10.1029/2003JD004030, 2004.
Noel, V. and Chepfer, H.: Study of ice crystal orientation in cirrus clouds based on satellite polarized radiance measurements, J. Atmos. Sci., 61, 2073–2081, 2004.
Noel, V., Winker, D., McGill, M., and Lawson, P.: Classification of particle shapes from lidar depolarization ratio in convective ice clouds compared to in situ observations during CRYSTAL-FACE, J. Geophys. Rev., 109, D24213, doi:10.1029/2004JD004883, 2004.
Platt, C. M. R.: Lidar and Radiometric observations of cirrus clouds, J. Atmos. Sci., 30, 1191–1204, 1973.
Platt, C. M. R., Scott, J. C., and Dilley, A. C.: Remote sensing of high clouds. Part VI: Optical properties of midlatitude and tropical cirrus, J. Atmos. Sci., 44(4), 729–747, 1987.
Platt, C. M. R., Winker, D. M., Vaughan, M. A., and Miller, S. D.: Backscatter-to-extinction in the Top Layers of Tropical Mesoscale Convective Systems and in Isolated Cirrus from LITE observations,J. Appl. Met., 38, 1330–1345, 1999.
Spinhirne, J. D., Reagan, J. A., and Herman, B. M.: Vertical Distribution of Aerosol Extinction Cross-Section and Inference of Aerosol Imaginary Index in the Troposphere by Lidar Technique, J. App. Met., 19(4), 426–438, 1980.
Stephens, G. L., Tsay, S.-C., Stackhouse, P. W., and Flatau, P. J.: The relevance of the microphysical and radiative properties of cirrus clouds to climate and climate feedback, J. Atmos. Sci., 47, 1742–1753, 1990.
Winker, D. M., Pelon, J., and McCormick, M. P.: The CALIPSO mission: Spaceborne lidar for observation of aerosols and clouds, Proc. SPIE, 4893, 1–11, 2003.
Winker, D. M.: Accounting for Multiple Scattering in Retrievals from Space Lidar, Proc. SPIE, 5059, 128–139, 2003.

Wylie, D. P., Menzel, W. P., Woolf, H. M., and Strabala, K. L.: Four Years of Global Cirrus clouds statistics using HIRS, J. Clim., 7, 315–335, 1994.
Zwally, H. J., Schutz, B., Abdalati, W., Abshire, J., Bentley, C., Brenner, A., Bufton, J., Dezio, J., Hancock, D., Harding, D., Herring, T., Minster, B., Quinn, K., Palm, S., Spinhirne, J., and Tomasm, R.: ICESat's Laser Measurements of Polar Ice, Atmosphere, Ocean, and Land, J. Geodyn., 34, 405–445, 2002.

ACPD
6, 10649–10672, 2006

Table 1. Properties of each case of collocated observations from the CPL and CIN during CRYSTAL-FACE.

	28 July	29 July
Time of observation	22:45–23:00	20:01–20:12
WB-57 Altitude range	13.5–16 km	12.5–14 km

ACPD
6, 10649–10672, 2006

Table 2. Cloud optical depth τ obtained from integration of volume coefficient profiles from the CPL and CIN observations.

	28 July	29 July
From CPL observations	1.87	5.08
From CIN observations	1.67	4.74

ACPD
6, 10649–10672, 2006

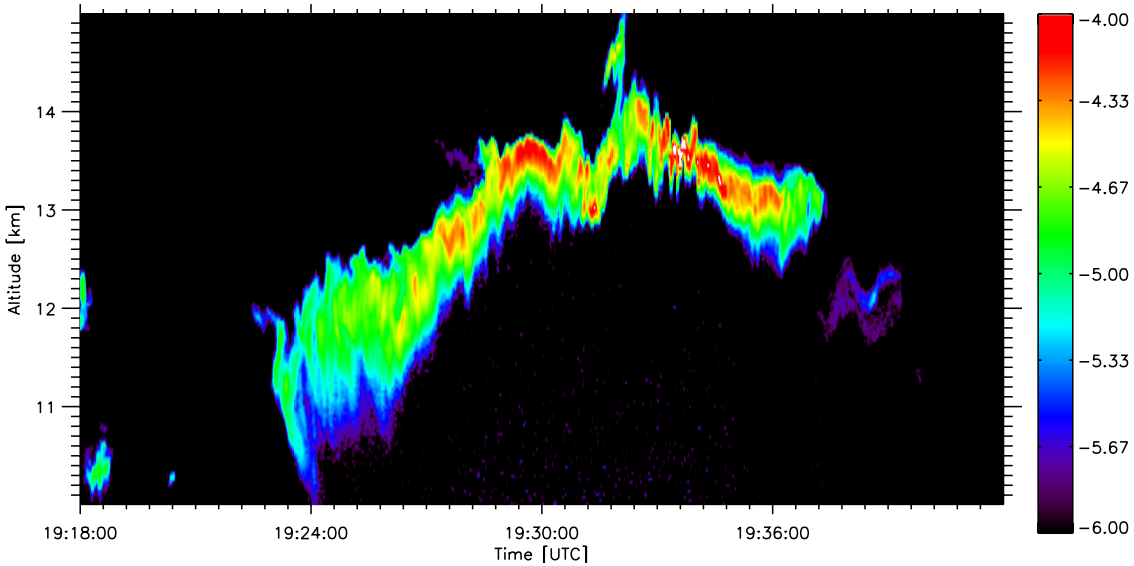

Fig. 1. Attenuated backscatter observed by the CPL as a function of time and altitude from 19:18 to 19:42 on 29 July 2002, using a logarithmic color scale (arbitrary units).

ACPD
6, 10649–10672, 2006

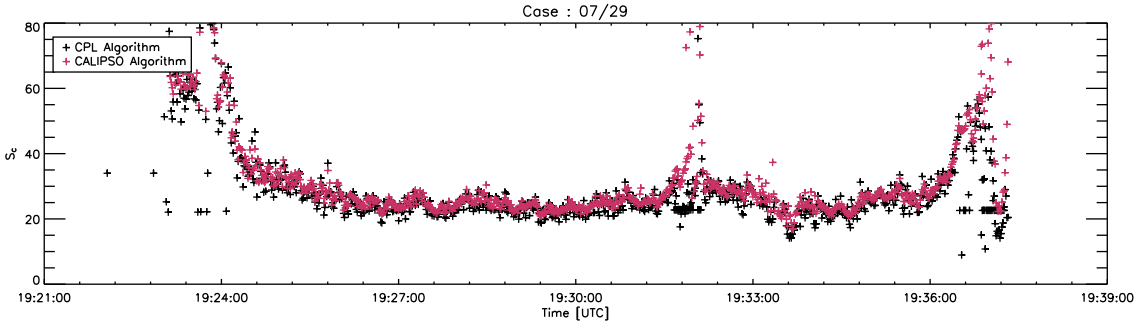

Fig. 2. Lidar ratios *S* for the same time period shown in Fig. 1, using the CPL retrieval algorithm (black) and the CALIPSO Deep Convection algorithm (red).

ACPD
6, 10649–10672, 2006

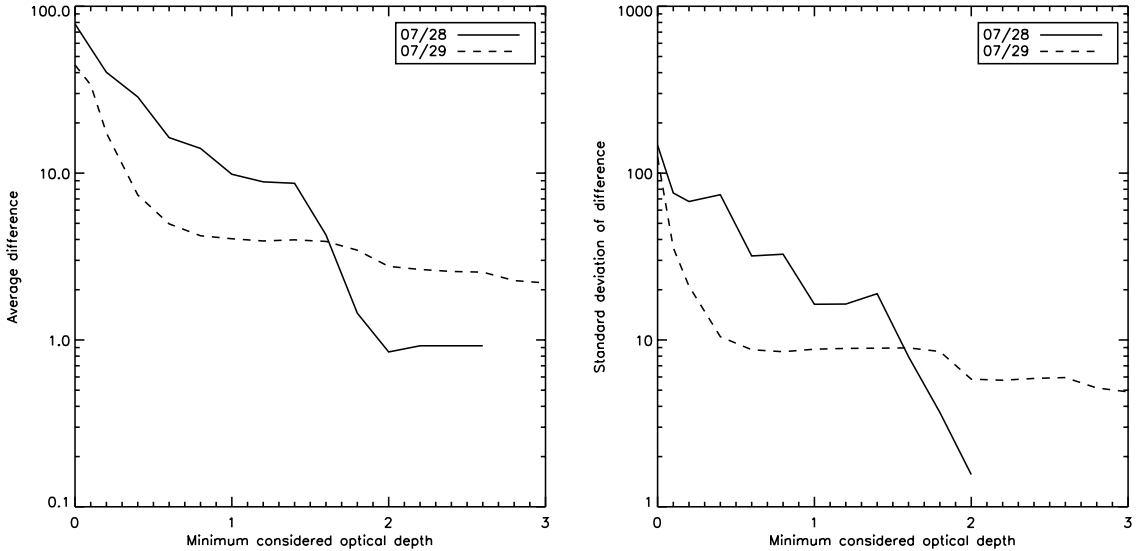

Fig. 3. Difference between lidar ratio *S* values retrieved using the CALIPSO Deep Convection algorithm and the CPL retrieval algorithm: average (left), standard deviation (right) as a function of the minimum considered optical depth.

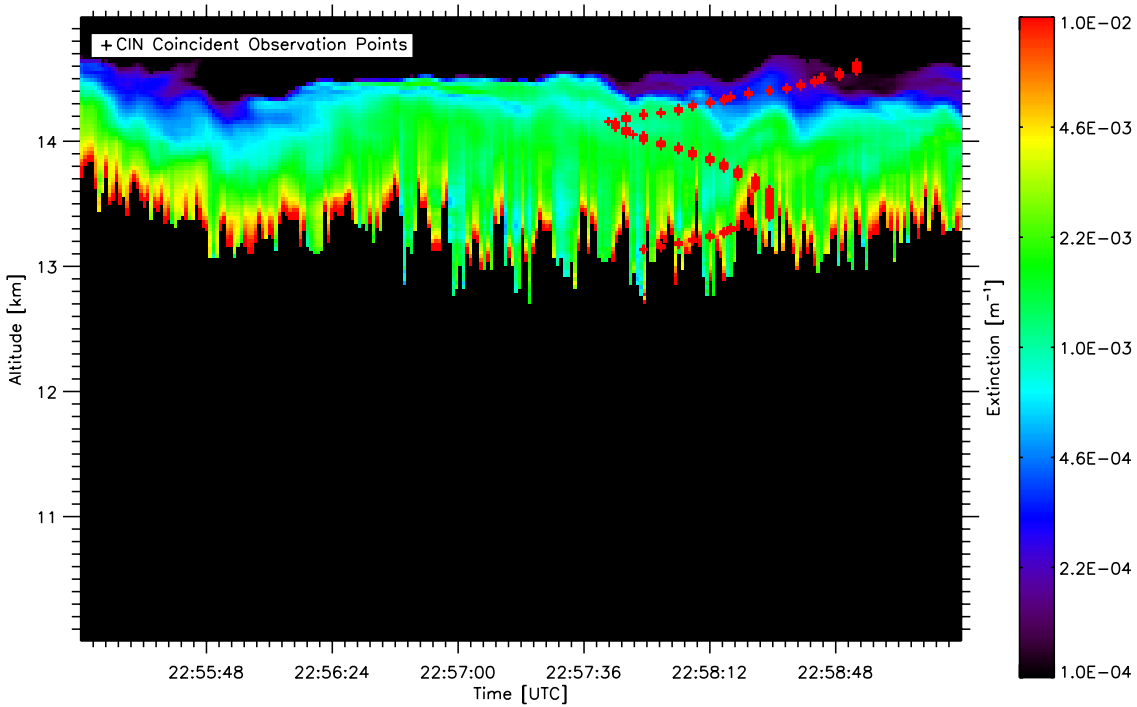

Fig. 4. Extinction (m^{-1}) retrieved from CPL backscatter observations and lidar ratio from the CALIPSO algorithm, between 22:55 and 23:00 on 28 July 2002, using a logarithmic color scale. The path of the WB-57, carrying the CIN probe, is plotted in red.

ACPD
6, 10649–10672, 2006

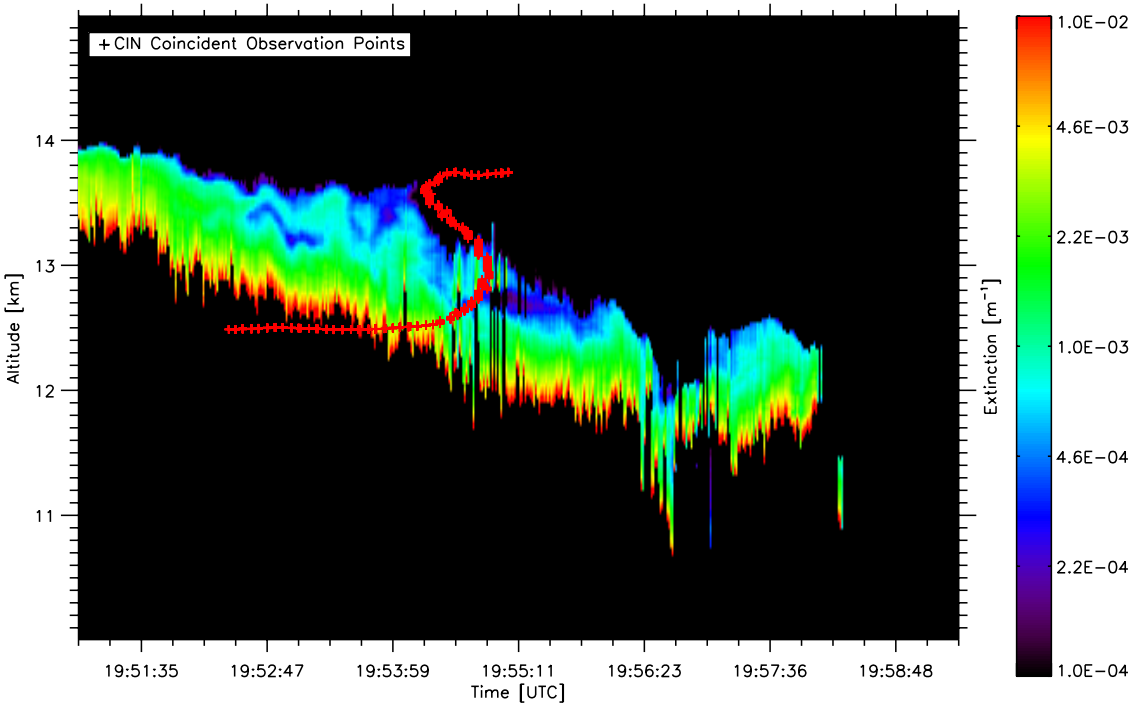

Fig. 5. Same as Fig. 4, for 29 July 2002 between 19:45 and 19:59.

ACPD
6, 10649–10672, 2006

EGU

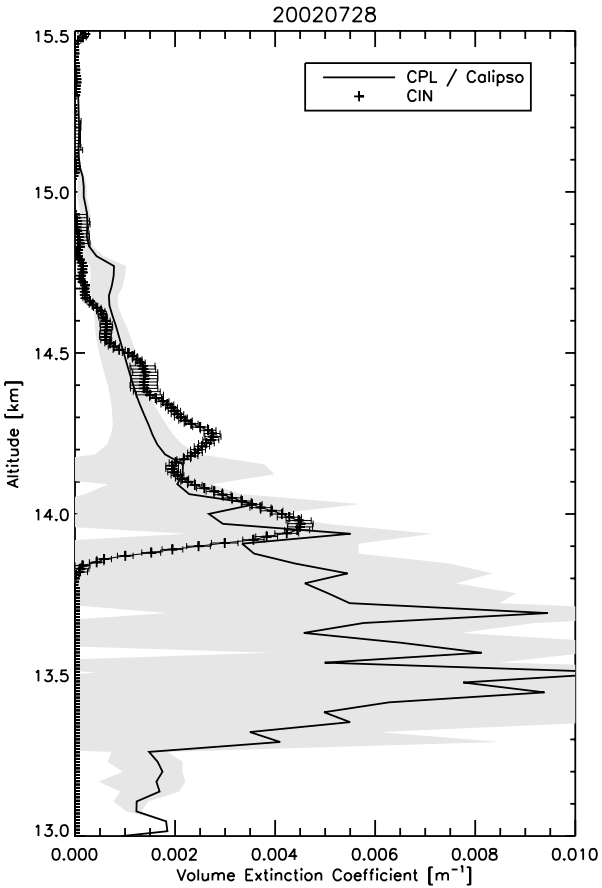

Fig. 6. Profile of extinction coefficients (m^{-1}) retrieved from CPL observations using the CALIPSO Deep Convection algorithm (average profile in full line, standard deviation in shaded grey) and from CIN collocated observations (crosses, with instrument uncertainty shown as horizontal bars) for the 28 July case, as a function of altitude (km).

ACPD
6, 10649–10672, 2006

EGU

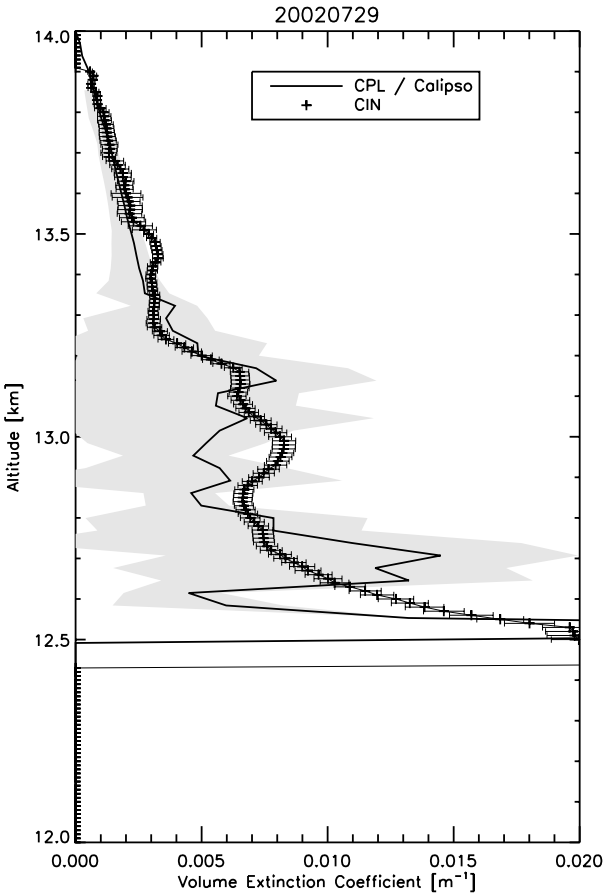

Fig. 7. Same as Fig. 6, for the 29 July case.

ACPD
6, 10649–10672, 2006